BMC Medical Imaging

RESEARCH

Open Access

Application value of CT three-dimensional reconstruction technology in the identification of benign and malignant lung nodules and the characteristics of nodule distribution

Guanghai Ji[1†], Fei Liu[1†], Zhiqiang Chen[2], Jie Peng[1], Hao Deng[3], Sheng Xiao[1*] and Yun Li[1*]

Abstract

Objective The study aimed to evaluate the application value of computed tomography (CT) three-dimensional (3D) reconstruction technology in identifying benign and malignant lung nodules and characterizing the distribution of the nodules.

Methods CT 3D reconstruction was performed for lung nodules. Pathological results were used as the gold standard to compare the detection rates of various lung nodule signs between conventional chest CT scanning and CT 3D reconstruction techniques. Additionally, the differences in mean diffusion coefficient values and partial anisotropy index values between male and female patients were analyzed.

Results Pathologic confirmation identified 30 patients with benign lesions and 45 patients with malignant lesions. CT 3D reconstruction demonstrated higher diagnostic accuracy for lung nodule imaging signs compared to conventional CT scanning ($P < 0.05$). The mean diffusion coefficient values and partial anisotropy index values were lower in female patients compared to male patients in the lung nodule lesion area, lung perinodular edema area, and normal lung tissue ($P < 0.05$). Conventional CT scanning showed a benign accuracy rate of 63.33% and a malignant accuracy rate of 60.00%, whereas CT 3D imaging achieved a benign and malignant accuracy rate of 86.67% for both. The accuracy rates for CT 3D imaging were significantly higher than those for conventional CT scanning ($P < 0.05$).

Conclusion CT 3D imaging technology demonstrates high diagnostic accuracy in differentiating benign from malignant lung nodules.

Keywords Computed tomography, Lung nodules, Lung tumors, Thoracic tumors, Diagnostic imaging

[†]Guanghai Ji and Fei Liu contributed equally to this work.

*Correspondence:
Sheng Xiao
Xiaosheng8188xs@163.com

[1]Department of Radiology, The First Affiliated Hospital of Yangtze University, No. 40 Jinlong Road, Shashi District, Jingzhou, Hubei 434000, China
[2]Department of Radiology, The First Hospital Affiliated of Hainan Medical University, Haikou, Hainan 570102, China
[3]Department of Urology, The First Affiliated Hospital of Yangtze University, Jingzhou, Hubei 434000, China

Introduction

Lung nodules are defined as homogeneous regions that contrast with the highly scattered dispersed lung parenchyma, which contains millions of air-filled alveoli [1]. The detection of lung nodules is a concerning issue for both patients and physicians, and it is crucial to distinguish those with high potential for malignancy [2]. The differentiation between benign and malignant lung nodules remains a diagnostic challenge [3]. Current medical imaging techniques are known to have a high false positive rate in identifying the nodules [4]. Therefore, developing an accurate method for differentiating solitary lung nodules is of paramount importance [5].

Computed tomography (CT) is a primary tool used in the clinical differentiation of benign and malignant lung nodules. Early classification of lung nodules is of great significance as it can slow down degenerative process and decrease mortality [6]. With rapid advancements in detection technologies, CT imaging is clinically widely utilized in the early diagnosis of lung nodules [7]. CT has proven to be an effective tool in the detection and characterization of lung nodules in vivo. Noninvasive methods possess, such as CT, have potential to alleviate clinical burdens, reduce risks, and lowered the costs related to further procedures [8]. The accurate differentiation of malignant lung nodules on chest CT is important in detecting lung cancer at an early stage and further offering patients with better chances of treatment and improved outcomes [9]. Recently, the use of CT three-dimensional (3D) reconstruction technology is growing in the preoperative planning of ground-glass nodule patients. The technique provides an economical and convenient method for more precise localization of lung lesions, which makes lung segment resection more accurate [10]. CT images combined with 3D reconstruction/printing models have shown a 100% agreement rate with pathological results, which aid in the precise and rapid localization of nodules in resected specimens. Moreover, the pathological results of lesions exhibit a high degree of agreement with preoperative CT imaging findings, which holds significant potential for future studies to investigate the clinicopathological characteristics of multiple lung nodules [11]. Inspired by the above findings, we aimed to explore the role of CT 3D reconstruction technology in differentiating benign from malignant lung nodules. Specifically, we sought to compare conventional CT scan and CT 3D reconstruction technology in identifying imaging signs, such as the burr sign, spinous protuberance, pleural indentation sign, vascular convergence sign, and small calcification sign. We also investigated the average diffusion coefficient and anisotropy index of pulmonary nodules in male and female patients, with a focus on the potential application value of CT 3D reconstruction technology in identifying benign and malignant lung nodules and understanding nodule distribution characteristics.

Materials and methods

Ethics statement

The study was approved by the Ethics Committee of the First Affiliated Hospital of Yangtze University (approval number: 20210915) and confirmed the Helsinki Declaration. Clinical trial number: ChiCTR2100120326.

General data

The retrospective, case-control study invited 100 patients who underwent chest CT scans at the First Affiliated Hospital of Yangtze University between December 2021 to June 2023. 75 patients with lung nodules were included in the study after exclusions (Fig. 1). The cohort consisted of 43 males and 32 females, with a mean age of 56.76±6.27 years and a disease duration of 1.89±0.34 years. CT 3D reconstruction of lung nodules, including coronal, sagittal, and VR images was performed at the workstation.

Exclusion and inclusion criteria

Inclusion criteria: (1) patients with a single solid lung nodule smaller than 30 mm in diameter. (2) patients with clear pathological findings; (3) patients without distant metastases on examination.

Exclusion criteria: (1) patients with multiple lung nodules or nodules located in more than in one lobe, requiring resection of multiple lobes; (2) patients who had received anti-tumor therapy before surgery; (3) patients with a history of malignancy; (4) patients with unclear pathological diagnoses; (5) patients with poor quality CT images or incomplete data.

Methods

Chest CT: Philips Core 128-slice CT scanner served as the instrument. The patient was positioned supine with arms raised above the head, removing any metal objects. The patient was instructed to inhale and then hold their breath before the scan began. The scan covered the lungs, starting from the apices to the base and from the thoracic entrance to the rib-diaphragm angle. The following parameters were applied: voltage 120 kV, scan thickness 5 cm, pitch 1.375, reconstruction interval 0.625 mm, lung window size (-700, 1000), and matrix 512×512.

After the routine scan, the data were collected and uploaded to the Philips workstation system for processing. Reconstruction results were recorded (Fig. 2). CT 3D reconstruction results were analyzed by three experienced imaging physicians with intermediate or higher qualifications. Representative images of benign and

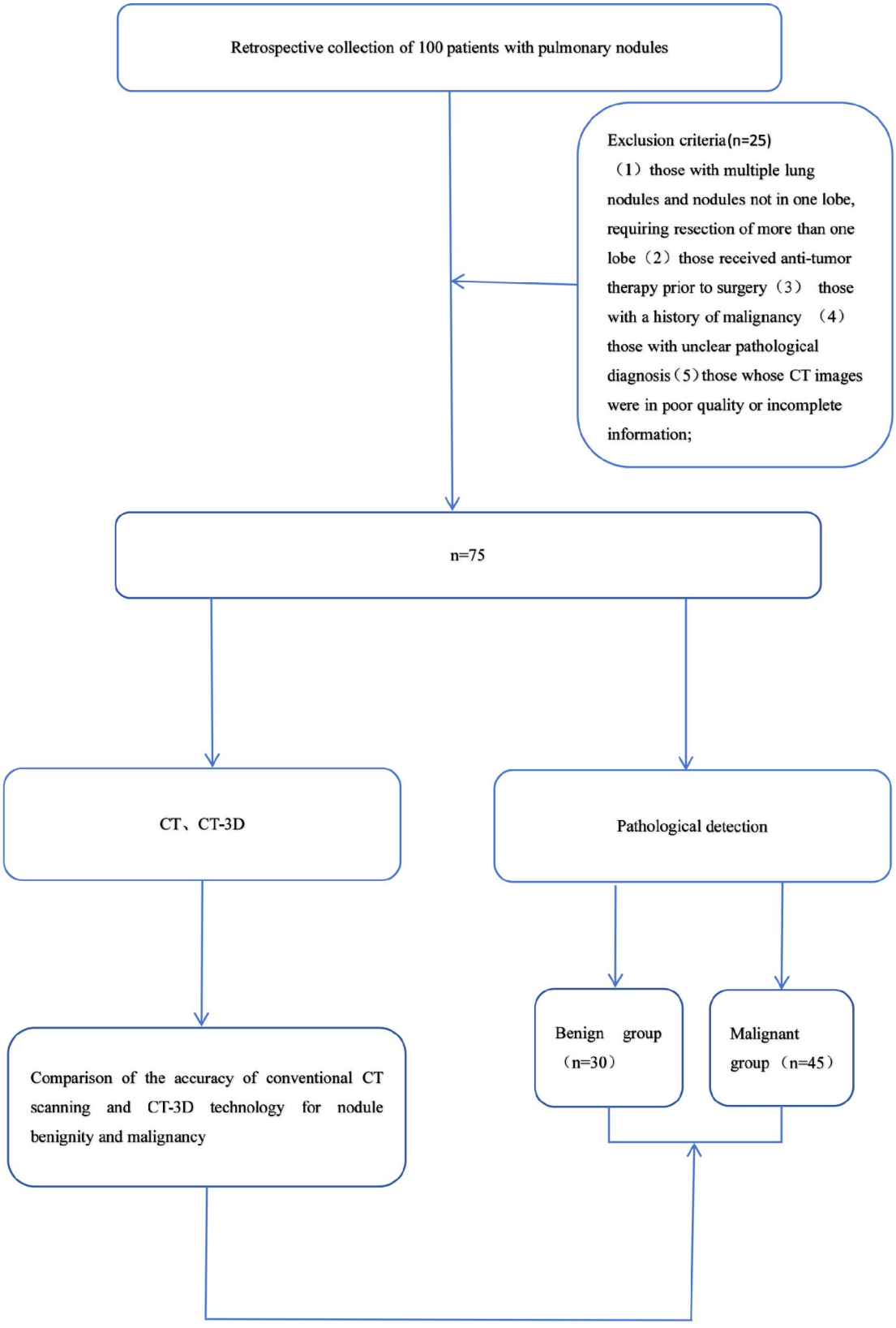

Fig. 1 Flow diagram of patient selection processes

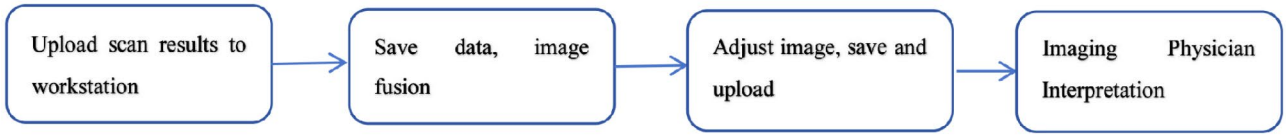

Fig. 2 Flow diagram of data analysis for CT 3D reconstruction

malignant nodules using conventional CT and CT 3D imaging were shown in Fig. 3.

Pathological assessment

All patients underwent pneumonectomy, and the appropriate surgical procedure was determined based on the number, size, and location of the nodules on chest CT 3D reconstruction. Postoperative specimens were subjected to routine pathological examination. A total of 75 patients were pathologically confirmed, with 30 benign lesions and 45 malignant lesions.

Observation indicators

We compared the diagnostic accuracy of conventional chest CT and CT 3D reconstruction technology using pathological findings as the "gold standard". The imaging characteristics and location distribution of lung nodules were obtained, and the detection rates of various lung nodule signs (such as nodule diameter, lobular sign, burr sign, pleural indentation sign, and vascular convergence sign) were compared. Differences in mean diffusion coefficient values and partial anisotropy index values between male and female patients were also recorded.

Statistics

GraphPad Prism 8.0 software (GraphPad Inc., La Jolla, CA, USA) was used for data analysis. Measurement data are expressed as mean ± standard deviation ($\bar{x} \pm$ sd) and analyzed using t-tests. Nominal data were analyzed using the chi-square test and presented as percentages (%). Differences were considered statistically significant when $P<0.05$.

Results

General clinical data

General clinical data, such as age, gender, smoking and drinking history, nodule diameter, and nodule location did not differ significantly between the benign and malignant groups ($P>0.05$) (Table 1).

Diagnostic accuracy of imaging signs between conventional CT scan and CT 3D imaging technology

CT 3D imaging technology demonstrated superior diagnostic accuracy compared to conventional CT scans in assessing burr signs, spinous protuberance, pleural indentation signs, vascular convergence signs, and small calcification signs ($P<0.05$) (Table 2).

Mean diffusion coefficient values between male and female patients

Female patients exhibited lower mean diffusion coefficient values for the lung nodule lesion part, lung perinodular edema part, and normal lung tissue part compared to male patients ($P<0.05$) (Table 3).

Anisotropy index values of lung nodular lesions between male and female patients

The anisotropy index values for the lung nodule lesion part, lung perinodular edema part, and normal lung tissue part were lower in female patients than in male patients ($P<0.05$) (Table 4).

Accuracy of conventional CT scan and CT 3D imaging technology for nodule benignity and malignancy

Conventional CT scanning exhibited a benign accuracy rate of 63.33% and a malignant accuracy rate of 60.00%. In contrast, CT 3D imaging demonstrated a benign accuracy rate of 86.67% and a malignant accuracy rate of 86.67%. Both benign and malignant accuracy rates of CT 3D imaging surpassed those of conventional CT scanning ($P<0.05$) (Table 5).

Discussion

Lung nodule evaluation aims to expediting the diagnosis and treatment of patients with malignant nodules while minimizing unnecessary diagnostic procedures for benign nodules [12]. The paper aimed to explore the application value of CT 3D reconstruction technology in the identification of benign and malignant lung nodules and in the examination of nodule distribution characteristics.

In the paper, we compared the diagnostic accuracy of imaging signs between conventional CT scans and CT 3D imaging technology. We found that CT 3D imaging offered higher diagnostic accuracy than conventional CT scans in detecting burr signs, spinous protuberance, pleural indentation signs, vascular convergence signs, and small calcification signs. Additionally, we compared the mean diffusion coefficient values and anisotropy index values of lung nodular lesions between male and female patients. Our results showed that female patients had lower mean diffusion coefficient values and anisotropy index values for the lung nodule lesion part, lung perinodular edema part, and normal lung tissue part compared to male patients. Furthermore, we evaluated

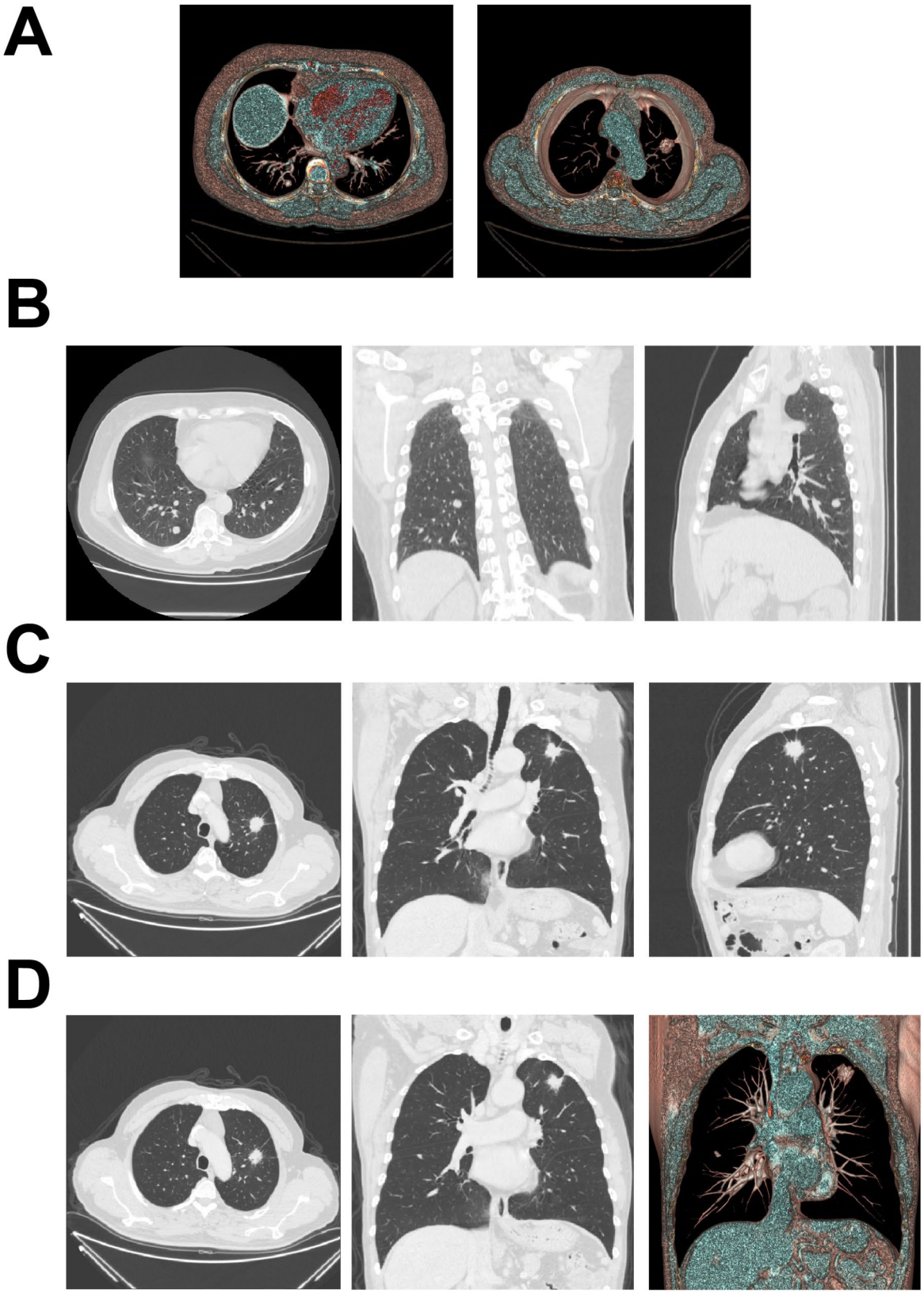

Fig. 3 CT 3D and conventional CT images of benign and malignant nodules. (**A**) CT-3D images. VR images of benign nodules (left) and malignant nodules (right); (**B**) CT scan images of transverse (left), coronal (middle) and sagittal (right) plane of benign nodules; (**C**) CT scan images of transverse (left), coronal (middle) and sagittal (right) plane of malignant nodules; (**D**) CT scan images of malignant burr signs (left), malignant pleural indentation signs (middle) and malignant vascular convergence signs (right)

Table 1 General clinical data

Data	The benign group ($n=30$)	The malignant group ($n=45$)	*P*
Gender			0.182
Male	20 (66.67)	23 (51.11)	
Female	10 (33.33)	22 (48.89)	
Age (years)	56.23 ± 6.45	57.11 ± 6.12	0.552
Smoking history			0.766
Yes	11 (36.67)	15 (33.33)	
No	19 (63.33)	30 (66.67)	
Drinking history			0.462
Yes	7 (23.33)	14 (31.11)	
No	23 (76.67)	31 (68.89)	
Nodule diameter			0.828
≤ 2	22 (73.33)	34 (75.56)	
> 2	8 (26.67)	11 (24.44)	
Nodule location			0.617
Upper lobes of the lung	21 (70.00)	29 (64.44)	
Middle/lower lobes of the lungs	9 (30.00)	16 (35.56)	

Table 2 Diagnostic accuracy of conventional CT scan and CT 3D imaging technology

Morphological characteristics	Conventional CT ($n=75$)	CT 3D imaging technology ($n=75$)	*P*
Burr sign	29 (38.67)	42 (56.00)	0.034
Spinous protuberance	7 (9.33)	16 (21.33)	0.041
Pleural indentation sign	10 (13.33)	22 (29.33)	0.017
Vascular convergence sign	3 (4.00)	11 (14.67)	0.025
Small calcification sign	4 (5.33)	12 (16.00)	0.034

Table 3 Mean diffusion coefficient values between male and female patients

Type	Male ($n=43$)	Female ($n=32$)	*P*
Lung nodule lesion part	1.33 ± 0.11	1.15 ± 0.03	< 0.001
Lung perinodular edema part	1.24 ± 0.04	0.93 ± 0.02	< 0.001
Normal lung tissue part	0.88 ± 0.09	0.72 ± 0.06	< 0.001

Table 4 Anisotropy index values of lung nodular lesion between male and female patients

Type	Male ($n=43$)	Female ($n=32$)	*P*
Lung nodule lesion part	0.17 ± 0.04	0.11 ± 0.03	< 0.001
Lung perinodular edema part	1.25 ± 0.07	0.16 ± 0.05	< 0.001
Normal lung tissue part	0.38 ± 0.04	0.32 ± 0.03	< 0.001

the accuracy of conventional CT scanning and CT 3D imaging technology in assessing nodule benignity and malignancy. Conventional CT scans had a benign accuracy rate of 63.33% and a malignant accuracy rate of 60.00%, whereas CT 3D imaging had a benign accuracy rate of 86.67% and a malignant accuracy rate of 86.67%, demonstrating the higher accuracy of CT 3D imaging technology.

The large volume of medical imaging data requires the use of advanced systems to reduce clinician workload [13] Image segmentation is a well-known image processing task that involves dividing an image into homogeneous regions [14], and it is widely adopted in medical fields for disease diagnosis [15–17] For instance, Garg S, Jindal B, et al. explored image processing techniques for the diagnosis of skin lesions, identifying an optimal method for segmenting skin lesion images, which enhances medical image processing systems [18–21]. The segmentation of the left ventricle in cardiac magnetic resonance images is crucial for accurate diagnosis [22]; similarly, the segmentation of abdominal CT scans is essential for analyzing, diagnosing, and treating disorders of internal organs, such as hepatocellular carcinoma [23]; in addition, the segmentation of real-time liver ultrasound is crucial for diagnosing and analyzing liver conditions (e.g., hepatocellular carcinoma), and assisting surgeons and radiologists in therapeutic procedures. Accurate segmentation of lung lesions from CT images is also essential for analyzing and diagnosing lung diseases. However, accurate lung nodule segmentation is challenging due to the small size and variety of lung nodules and, the lack of high-quality markers [24]. Therefore, advanced segmentation techniques, combined with traditional and machine learning algorithms, can help classify nodules based on patterns learned from large datasets. These algorithms can be trained to identify patterns associated with benign or malignant nodules, thus improving diagnostic accuracy. In the medical field, combined use of image segmentation and CT 3D reconstruction can significantly enhance diagnosis accuracy and efficiency.

As previously reported, lung nodules are detected in about 30% of chest CT images [25]. CT is also the first choice for diagnosing solid solitary lung nodules. The clarification of differential CT characteristics based on diameter ranges may reduce ambiguities and help distinguishing the benign solid solitary lung nodules from

Table 5 Accuracy of conventional CT scan and CT 3D imaging technology for nodule benignity and malignancy

Diagnostic results		Conventional CT		CT 3D image technology		Total
		Benignity	Malignancy	Benignity	Malignancy	
Case criteria	Benignity	19 (63.33)	11 (36.67)	26 (86.67)*	4 (13.33)	30
	Malignancy	18 (40.00)	27 (60.00)	6 (13.33)	39 (86.67)*	45
Total		37	38	32	43	

Note: * $P<0.05$ vs. conventional CT

malignant ones [26]. The use of 3D measurements during follow-up for lung ground glass nodules is of increasing significance [27]. Previous studies have shown that CT multi-plane 3D reconstruction navigation can promote the diagnostic efficiency of radial endobronchial ultrasound for solitary lung nodules, and combined CT multi-plane 3D reconstruction with radial endobronchial ultrasound improves diagnostic values for peripheral solitary lung nodules [28]. Moreover, the 3D convolution neural network has demonstrated efficiency in the identification of benign and malignant lung nodules using various CT reconstruction classification algorithms [29]. Meanwhile, 3D reconstruction combined with dial positioning methods has shown acceptable accuracy and holds promise for further clinical promotion and application [30]. The 3D gray density coding feature can provide more accurate results for the classification of benign and malignant lung nodules, and offer additional support for clinicians [31]. Thus, CT 3D reconstruction technology holds considerable value in differentiating benign from malignant lung nodules.

In summary, the research demonstrates that CT 3D imaging technology has significant application value and high diagnostic accuracy in the identification of benign and malignant lung nodules, especially small ones. CT 3D reconstruction can clearly, accurately, and intuitively display the morphology, internal structure, edge boundaries, and surrounding tissue structures of nodular lesions, which substantially enhances the ability to distinguish between benign and malignant pulmonary nodules. The technology offers value in preoperative evaluation, surgical planning, identification of pulmonary vessels and bronchi during surgery, and guiding teaching. It is suitable for clinical implementation and development. As the technology continues to mature, it may improve the accuracy of pulmonary nodule resections. The study lays the foundation for further exploration of the clinical application of CT 3D reconstruction technology in identifying benign and malignant lung nodules. Nevertheless, our study has some limitations. For example, there may be subjective differences in interpreting 3D reconstructed images, and our data derived rom a single center, which could lead to selection bias. Moreover, the sample size and representation were limited. Further high-quality studies are needed to address the limitations and promote the area of research.

Acknowledgements
We would like to express our sincere gratitude to the reviewers for their constructive comments.

Author contributions
G.H.J and F.L. contributed the study design, Z.Q.C. and J.P. conducted the experimental studies, H.D. and S.X. performed the data analysis, and Y.L. was responsible for manuscript editing. All authors read and approved the final version of the manuscript.

Funding
The work was not funded by any organization.

Data availability
No datasets were generated or analysed during the current study.

Declarations

Ethics approval and consent to participate
All patients provided informed consent and signed a written informed consent form. The study was approved by the Ethics Committee of the First Affiliated Hospital of Yangtze University (approval number: 20210915) and adhered to the Helsinki Declaration. Clinical trial number: ChiCTR2100120326.

Consent for publication
Not applicable.

Competing interests
The authors declare no competing interests.

Received: 28 May 2024 / Accepted: 18 November 2024
Published online: 06 January 2025

References

1. Roshankhah R, Blackwell J, Ali MH, Masuodi B, Egan T, Muller M. Detecting pulmonary nodules by using ultrasound multiple scattering. J Acoust Soc Am. 2021;150(6):4095.
2. Popovic K, Miladinovic M, Vuckovic L, Nedovic M, Vukovic. Rare benign lung tumours presenting with high clinical suspicion for malignancy: a case series and review of the literature. Folia Histochem Cytobiol. 2023;61(2):130–42.
3. Zhang B, Liang H, Liu W, Zhou X, Qiao S, Li F, et al. A novel approach for the non-invasive diagnosis of pulmonary nodules using low-depth whole-genome sequencing of cell-free DNA. Transl Lung Cancer Res. 2022;11(10):2094–110.
4. Xie C, Huang Q, Liu Y. Utility of peripheral blood macrophage factor Apo10 and TKTL1 as markers in distinguishing malignant from benign lung nodules: a protocol for a prospective cohort study in Southern China. BMJ Open. 2023;13(11):e076573.
5. Jacob M, Romano J, Ara Jo D, Pereira JM, Ramos I, Hespanhol V. Predicting lung nodules malignancy. Pulmonology. 2022;28(6):454–60.
6. Zhu H, Liu W, Gao Z, Zhang H. Explainable classification of Benign-Malignant Pulmonary nodules with neural networks and information bottleneck. IEEE Trans Neural Netw Learn Syst; 2023.
7. Lv E, Liu W, Wen P, Kang X. Classification of Benign and malignant lung nodules based on deep Convolutional Network feature extraction. J Healthc Eng. 2021;2021:p8769652.
8. Uthoff J, Stephens MJ, Newell JD Jr., Hoffman EA, Larson J, Koehn N, et al. Machine learning approach for distinguishing malignant and benign lung nodules utilizing standardized perinodular parenchymal features from CT. Med Phys. 2019;46(7):3207–16.
9. Xie Y, Xia Y, Zhang J, Song Y, Feng D, Fulham M, et al. Knowledge-based Collaborative Deep Learning for Benign-Malignant Lung Nodule classification on chest CT. IEEE Trans Med Imaging. 2019;38(4):991–1004.
10. Zhao X, Lu H, Zhang Z. [Preliminary study of CT three-dimensional Reconstruction combined with Ground Glass Nodules of Natural Lung Collapse in Thoracoscopic Pulmonary Segmental Resection]. Zhongguo Fei Ai Za Zhi. 2021;24(10):683–9.
11. Ji Y, Zhang T, Yang L, Wang X, Qi L, Tan F, et al. The effectiveness of three-dimensional reconstruction in the localization of multiple nodules in lung specimens: a prospective cohort study. Transl Lung Cancer Res. 2021;10(3):1474–83.
12. Sethi S, Cicenia J. Role of biomarkers in lung nodule evaluation. Curr Opin Pulm Med. 2022;28(4):275–81.
13. Dakua SP, Sahambi JS. *LV Contour Extraction from Cardiac MR Images Using Random Walks Approach*.. IEEE international advance computing conference, 2009. pp. 228–233.
14. Cardone B, Di Martino F, Miraglia V. A novel fuzzy-based remote sensing image Segmentation Method. Sens (Basel), 2023. 23(24).

15. Ansari MY, Yang Y, Meher PK, Dakua SP. Dense-PSP-UNet: a neural network for fast inference liver ultrasound segmentation. Comput Biol Med. 2022;153:106478.
16. Dakua SP, Sahambi JS. Detection of left ventricular myocardial contours from ischemic cardiac MR images. Iete J Res. 2011;57(4):372–84.
17. Ansari MY, Chandrasekar V, Singh AV, Dakua SP. Re-routing drugs to blood brain barrier: a comprehensive analysis of machine learning approaches with fingerprint amalgamation and data balancing. IEEE Access. 2022;11:9890–906.
18. Garg S, Jindal B. Skin lesion segmentation using k-mean and optimized fire fly algorithm. Multimed Tools Appl. 2021;80:7397–410.
19. Garg S, Jindal B. Skin lesion segmentation in Dermoscopy Imagery. Int Arab J Inf Technol. 2022;19(1):29–37.
20. Garg S, Jindal B. FDLM: an enhanced feature based deep learning model for skin lesion detection. Multimed Tools Appl. 2024;83(12):36115–27.
21. Jindal B, Garg S. FIFE: fast and indented feature extractor for medical imaging based on shape features. Multimed Tools Appl. 2023;82(4):6053–69.
22. Dakua SP, Sahambi JS. Automatic left ventricular contour extraction from cardiac magnetic resonance images using cantilever beam and random walk approach. Cardiovasc Eng. 2010;10(1):30–43.
23. Ansari MY, Yang Y, Balakrishnan S, Abinahed J, Al-Ansari A, Warfa M, et al. A lightweight neural network with multiscale feature enhancement for liver CT segmentation. Sci Rep. 2022;12(1):14153.
24. Wang C, Xu R, Xu S, Meng W, Xiao J, Zhang X. Accurate lung nodule segmentation with detailed representation transfer and soft Mask Supervision. IEEE Trans Neural Netw Learn Syst; 2023.
25. Mazzone PJ, Lam L. Evaluating the patient with a pulmonary nodule: a review. JAMA. 2022;327(3):264–73.
26. He XQ, Huang XT, Luo TY, Liu X, Li Q. The differential computed tomography features between small benign and malignant solid solitary pulmonary nodules with different sizes. Quant Imaging Med Surg. 2024;14(2):1348–58.
27. Zhou Y, Zhang Y, Zhang S, Zhang C, Chen Z. [Growth regularity of Pulmonary Ground Glass nodules based on 3D Reconstruction Technology]. Zhongguo Fei Ai Za Zhi. 2023;26(4):265–73.
28. Wang W, Zhan P, Xie Q, Hu HD, Wang YC, Yuan Q, et al. [Combination of CT mulitplane 3D reconstruction, radial endobronchial ultrasound and rapid on-site evaluation for diagnosing peripheral solitary pulmonary nodules]. Zhonghua Yi Xue Za Zhi. 2019;99(2):93–8.
29. Lu Z, Long F, He X. *Classification and Segmentation Algorithm in Benign and Malignant Pulmonary Nodules under Different CT Reconstruction.* Comput Math Methods Med, 2022. 2022: p. 3490463.
30. Zhao L, Yang W, Hong R, Fei J. Application of three-dimensional reconstruction combined with dial positioning in small pulmonary nodules surgery. J Cardiothorac Surg. 2021;16(1):254.
31. Zheng B, Yang D, Zhu Y, Liu Y, Hu J, Bai C. 3D gray density coding feature for benign-malignant pulmonary nodule classification on chest CT. Med Phys. 2021;48(12):7826–36.

Publisher's note